RESEARCH ARTICLE

Effects of Contact Tracing and Self-Reporting in a Network Disease Model

Punit Gandhi, Michael A. Robert, John Palacios, David Chan

Department of Mathematics and Applied Mathematics, Virginia Commonwealth University, Richmond, VA

ABSTRACT

We examine the effects of symptomatic individuals getting tested and the use of contact tracing in a network model of disease transmission on different epidemiological metrics. These metrics include the length of the epidemic, number of people infected, number of tests performed, and the likelihood of an epidemic occurring. We utilize a network model to resolve the influence of contact patterns between individuals as opposed to assuming mass action where all individuals are connected to each other. We find that the effects of self-reporting and contact tracing vary depending on the structure of the network. We also compare the results from the network model with an analogous ODE model that assumes mass action and demonstrate how the results can be dramatically and surprisingly different.

1 Introduction

Contact tracing is an important intervention strategy for controlling an infectious disease outbreak that is aimed at determining with whom a known infectious person has recently been in contact. Those individuals that have been in recent contact with the infected individual are then notified, quarantined, and tested. Contact tracing can require substantial investments in time, money, and personnel in order to be successful, but there are a number of precedents for the utility of contact tracing in infectious disease management. First introduced in the United States in the 1930s in attempt to control the spread of syphilis, contact tracing has proven to be an effective method for the control of sexually transmitted infections (STIs) (Ramstedt et al., 1990; Cowan et al., 1996). Contact tracing has been an important component to control efforts of emerging infectious diseases in localized settings such as severe acute respiratory syndrome (SARS), Ebola, and Nipah virus (Dhillon and Srikrishna, 2018; Donnelly et al., 2003; World Health Organization et al., 2014; Arunkumar et al., 2019). Most recently, contact tracing has been included among a suite of non-pharmaceutical interventions (NPIs) in efforts to control the spread of severe acute respiratory syndrome coronavirus 2 (SARS-CoV-2), the causative agent of COVID-19 (WHO, 2020; Steinbrook, 2020; MacIntyre, 2020).

In order for contact tracing to be effective, infected individuals must self-report and get tested to determine whether they are infectious thereby initiating the contact tracing process. This becomes more difficult in diseases that involve asymptomatic individuals, who generally would not self-report due to the lack of symptoms. An alternate approach is to carry out surveillance testing across a population or even mandate testing for all individuals.

It is challenging for public health policy makers to make decisions about intervention methods. It can also be challenging for modelers to choose the types of models that can provide accurate results to base these decision upon. Mathematical models have been used to better understand the potential efficacy of contact tracing in infectious disease control and to help optimize the contact tracing process (Müller and Kretzschmar, 2021; Eames and Keeling, 2003; Hyman et al., 2003; Hethcote and Yorke, 2014). Models used to study contact tracing vary in structure and complexity from relatively simple ordinary differential equation (ODE) models mimicking the impacts of contact tracing to agent-based models (ABMs) that track individuals and their contacts explicitly (Müller and Kretzschmar, 2021). A number of studies have looked at contact tracing in combination with other control measures. Klinkenberg et al. (2006) employed an ODE model investigating the balance between regular screening and contact tracing. They determined that contact tracing is only cost effective when disease prevalence is below a certain threshold. Armbruster and Brandeau (2007) utilized a branching process model that included isolation and social distancing to show that the efficacy of contact tracing may be a function of timing between infections, duration of infections, and delays in testing.

Karaivanov (2020) considered an SIR model on a network, illustrating that measures such as lockdowns, quarantines, and social distancing may be better modeled on networks rather than in models where homogeneous mixing is assumed. Shaban et al. (2008) also employed a network model with SIR dynamics to investigate the efficacy of contact tracing alongside vaccination. Network models have been of particular use in contact tracing modeling studies and infectious disease modeling more generally in part because they allow for consideration of individuals and their contact structures, but do not have the same limitations in mathematical analysis that ABMs may have (Keeling and Rohani, 2011). Furthermore, numerous network approximation methods have been developed that allow for analysis and simulation of network models while still maintaining important characteristics of network structure (Tsimring and Huerta, 2003). In the context of diseases such as COVID-19 where NPIs such as social distancing have been important, network models can be particularly useful in understanding how spread and control dynamics change when individuals within the population change their behavior.

COVID-19 has renewed interest in contact tracing models and their utility in understanding the efficacy of different contact tracing methods. This work has led to exploration of new methods of contact tracing which may be more effective than traditional contact tracing approaches (Firth et al., 2020; Bradshaw et al., 2021). The works of both Firth et al. (2020) and Karaivanov (2020) looked more specifically at the role of social networks as these networks are more likely to incorporate frequent interactions among contacts, and access to healthcare resources may differ across different social networks. While not specifically considering contact tracing, Azizi et al. (2020) considered another important question specific to modern day infectious disease control: how does the rapid availability of information impact awareness of infectious disease transmission? Using a network model that mimics both infectious disease and information dynamics, they investigate how different thresholds of awareness impact epidemic dynamics.

Much of the recent work employing network models to investigate contact tracing have sparked a number of important questions that are relevant to the control of COVID-19 spread as well as the control of other directly transmitted diseases. For instance, how does the willingness to be tested affect the spread of the disease? How does the effectiveness of contract tracing impact diseases transmission? How might contact tracing play a role in the ability to prevent transmission and reduce outbreak size? How will these factors be affected by the structure of the network and other NPIs such as social distancing?

Herein, we aim to answer these questions in the context of directly transmitted diseases with an epidemiological model on a network. We investigate the importance of key variables such as rates of contact tracing, rates at which symptomatic individuals get tested, and the structural properties of the network on the ability of contact tracing to impact the spread of disease. These structural properties are related to how people are connected within the network and the effects of social distancing. We also emphasize the importance of this network structure by comparing the network model to an approximate ordinary differential equation (ODE) model. In the sections that follow, we describe our epidemiological model, network, and the interplay between the two, along with the ODE model. We present results for a number of scenarios that result from different parameter combinations, and discuss our results and their importance for control of directly transmitted diseases.

Some surprising conclusions that we observed in our simulations include that there exists a minimum threshold for contact tracing where the likelihood of outbreaks drops when above this threshold in the network model, whereas this does not occur in the ODE model. Also that the length of the epidemic has a reverse behavior with respect to the contact tracing rate where in the network model as the contact tracing rate increase the length of the epidemic decreases, and in the ODE model this is reversed. We find the lowest number of people infected in the network model occurs for high contract tracing rates and high self reporting rates. In the ODE model the lowest number of infections are found for low contact tracing rates and high self reporting rates. We also find that the highest number of test performed occurs at low contact tracing rates for the network model, whereas for the ODE model this occurs at high contact tracing rates. We also discuss the important differences in the results between the network model and the ODE model. These contrast in conclusions between these models is a direct result of the fact that mass action that is used as a simplifying assumptions in the ODE model.

2   Model Description

This section outlines two distinct models for exploring the impact of contact tracing and self-reporting on an epidemic: a stochastic network model and an ODE model. Our goal in this study is to demonstrate various behaviors within the network model and to highlight the significant differences in predictions relative to the ODE model. We divide the presentation of the epidemiological network model into two parts: Section 2.1 describes the disease dynamics of individuals and Section 2.2 describes the network structure that characterizes the interactions between individuals. In 2.3, we describe an ODE model that approximates mean-field dynamics of the disease spread.

The disease model expands upon a standard *SEIR*-type epidemic model that distinguishes between symptomatic and asymptomatic infections. It includes additional states to track individuals that are quarantined while their contacts are tested, as well as individuals that are tested and isolate themselves while awaiting results. Figure 1 summarizes the possible transitions between states for a given individual.
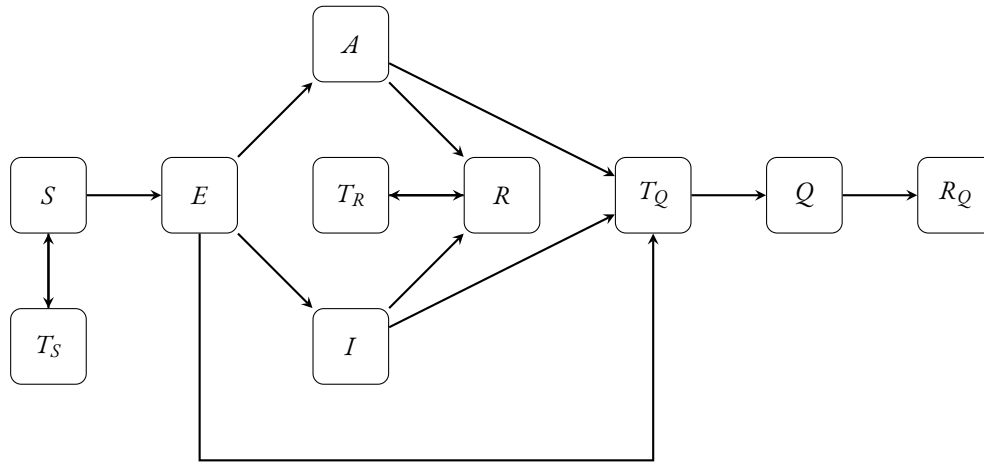
Figure 1: Schematic of transitions between states in the disease transition model: susceptible (S), exposed (E), symptomatic infected (I), asymptomatic infected (A), recovered (R), quarantined during contact tracing (Q), tested as susceptible (T_S), tested as recovered (T_R), those who are infected/asymptomatic and then tested (T_Q), and those who recover while quarantined (Q_R). Approximate transition probabilities are summarized in Table 1.

The disease model assumes that infected individuals can spread the disease through contact with others. The stochastic network model assumes a Watts-Strogatz random graph (Watts and Strogatz, 1998) to capture the structure of contacts between individuals. The ODE model, on the other hand, is valid for a well-mixed population (Kiss et al., 2017). In Section 3, we provide a comparison of the two modeling approaches, highlighting important distinctions between the predictions. The network approach has the advantage of explicitly capturing details of the contact between individuals by which the epidemic spreads and tracing is implemented.

2.1   Disease transmission model

We represent a population of interacting individuals as N nodes, each connected by edges to other nodes with whom they regularly come into contact. Each individual in the model is in one of the following states: susceptible (S), exposed (E), symptomatic infected (I), asymptomatic infected (A), recovered (R), quarantined (Q), tested as susceptible (T_S), tested as recovered (T_R), those who are exposed or infected (either symptomatic or asymptomatic) and then tested (T_Q), and those who recover while quarantined (R_Q). Each individual has a transition probability depending on the current state they are in and the destination state. These possible transitions are summarized by Figure 1 and the associated transition probabilities are presented in Table 1.

Infected individuals can either be symptomatic (I) or asymptomatic (A) and spread the disease to each of their susceptible (S) contacts with rate β. We note that this rate, as are all of the following rates we discuss, are given as probabilities per unit time. Successful spread of the disease is modeled by a transition from susceptible to exposed ($S \rightarrow E$). Exposed individuals become symptomatic with rate α_I, and asymptomatic with rate α_A. Once showing symptoms, symptomatic nodes choose to get tested ($I \rightarrow T_Q$) with rate σ and recover ($I \rightarrow R$) with rate γ_I.

The testing process for an infected symptomatic individual is modeled by a transition of the node to the state T_Q, whereupon the node isolates itself from contact with other nodes. Test results are returned with rate δ and the positive testing individuals transition to a quarantine state (Q) whereupon contact tracing begins. All of the contacts of the individual in quarantine are tested with rate τ until that node transitions out of quarantine and into a recovery state ($Q \rightarrow R_Q$), which occurs with rate γ_Q. All individuals tested during the contact tracing process will isolate from their contacts until the test results are returned. This is modeled by a transition of the individual to awaiting test results ($S \rightarrow T_S, R \rightarrow T_R, E \rightarrow T_Q, I \rightarrow T_Q, A \rightarrow T_Q$), followed by a transition either back to its original state or to the quarantine ($T_S \rightarrow S, T_R \rightarrow R, T_Q \rightarrow Q$) depending on the result of the test.

We assume the test accurately detects infections in exposed and infected individuals, and do not account for errors in test results. We assume perfect isolation of individuals while waiting for the test results in quarantine, and thus there is no chance for disease spread by any node in states T_Q or Q. We also assume recovered individuals in states R and R_Q cannot be reinfected, and are thus effectively removed from the epidemic process. Because there is no memory in a Markov process, the model does not rule out the possibility of a contact being tested multiple times during the contact tracing of an individual. We fix the rate for completion of the tracing process to $\gamma_Q = 0.5$. Thus, the quarantine period lasts for two days on average, and an increase in τ leads to an increase in the average number of contacts that can be tested during that period. All model parameters, along with

Table 1: Linear approximation to probability for a node in state S to make the transition to state Q, i.e. $S \to Q$, during a the time interval ΔT, given that it has $n_{\mathcal{P}}$ contacts in states $\mathcal{P}$. Figure 1 summarizes the possible states in the disease transition model.

Transition	Probability		Transition	Probability		Transition	Probability
$S \to E$	$(n_I + n_A)\beta\Delta T$		$I \to T_Q$	$(\sigma + n_Q\tau)\Delta T$		$S \to T_S$	$n_Q\tau\Delta T$
$E \to A$	$\alpha_A\Delta T$		$A \to T_Q$	$n_Q\tau\Delta T$		$T_S \to S$	$\delta\Delta T$
$E \to I$	$\alpha_I\Delta T$		$E \to T_Q$	$n_Q\tau\Delta T$		$R \to T_R$	$n_Q\tau\Delta T$
$A \to R$	$\gamma_A\Delta T$		$T_Q \to Q$	$\delta\Delta T$		$T_R \to R$	$\delta\Delta T$
$I \to R$	$\gamma_I\Delta T$		$Q \to R_Q$	$\gamma_Q\Delta T$			

Table 2: Typical parameter values for our disease transmission model summarized by Figure 1 and Table 1, and the Watts-Stogatz contact network model. The rates are given as probability per unit time in days^{-1}. Values were chosen to be consistent with those of directly transmitted infectious diseases.

Parameter	Value	Description	Reference(s)
β	0.05	Transmission rate per contact	Tupper et al., 2020
α_I	0.6	Rate for exposed to become symptomatic	Lessler et al., 2009 Cope et al., 2018 CDC, 2022a
α_A	0.1	Rate for exposed to become asymptomatic	Lessler et al., 2009 Cope et al., 2018
γ_I	0.1	Rate for symptomatic to recover	CDC, 2022a,b
γ_A	0.1	Rate for asymptomatic to recover	CDC, 2022a,b
γ_Q	0.5	Rate for tracing process completion	Kucharski et al., 2020
σ	0–1	Rate for symptomatic to choose to get tested	—
τ	0–1	Rate of testing contacts during tracing	—
δ	0.3	Rate for testing to be completed	Kucharski et al., 2020
κ	20, 40	Average degree of nodes in contact network	—
p	0.01, 0.1	Rewiring probability for edges in contact network	—

typical values, are given in Table 2. We note that parameter values were chosen not to reflect any specific disease; however, we assume that the pathogen can be transmitted via direct contact as is the case with many respiratory pathogens. The values we have chosen are consistent with diseases caused by viruses such as influenza, SARS-CoV, SARS-CoV-2, and adenovirus as cited from empirical and modeling literature. Parameters not obtained directly from literature, such as κ and p, were chosen to reflect markedly different contact structures so that we could emphasizes differences that result from these different structures.

We carry out the process outlined above as a discrete-time Markov chain and take the time step ΔT small enough in our numerical implementation so that all of the transition probabilities, summarized in Table 1, are well-approximated at order $O(\Delta T)$. In particular, we multiply the total number of infected symptomatic and asymptomatic contacts, $n_I + n_A$, by the per-contact probability rate of infection β to the approximate effective probability rate of infection for a given node. Similarly, the effective probability rate for a node to be tested from contact tracing is approximated by $n_Q\tau$, where n_Q is the number of quarantined contacts that node has. Simulation code for an implementation of this model in Matlab is available from GitHub (2022).

2.2   Network structure for contacts

We consider the stochastic disease transition model summarized by Figure 1 and Table 1 on a random graph were the N nodes represent individuals and edges represent regular contact between individuals. A Watts-Strogatz network is characterized by average node degree $\kappa = 2k$, for some natural number k, and rewiring probability $0 \leq p \leq 1$. The graph is generated by first constructing a regular ring network in which the nodes are all connected to k of their nearest neighbors on each side by an edge. The edges are then rewired with probability p. If chosen to be rewired, one of the two nodes associated with the edge is replaced by another chosen from the remaining nodes uniformly at random in such a way that there are no duplicates or self-edges. An

(a) $p = 0$ (b) $p = 0.01$ (c) $p = 0.1$
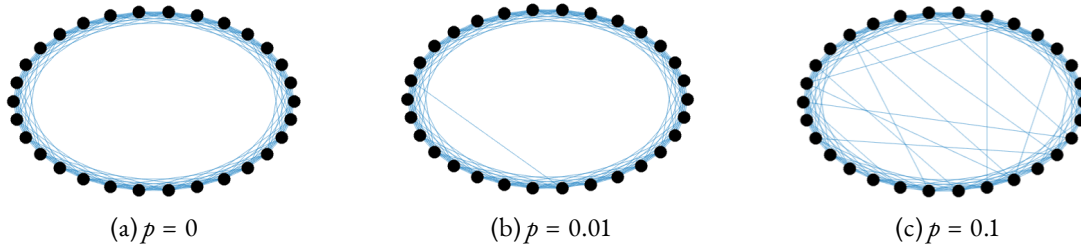
Figure 2: Watts-Stogratz networks represented as rings of $N = 30$ nodes and average degree of $\kappa = 10$. The rewiring probability p increases from left to right.

advantage of a Watts-Strogatz network structure in this setting is that it allows for two types of control: the parameters κ and p, which we relate to social distancing and connectivity in the network, respectively. See Figure 2 for examples with $N = 30$ nodes, average node degree $\kappa = 10$ and different values of the rewiring probability p.

The degree of a node is the number of other nodes that it comes into regular contact with, and thus measures the maximum number of nodes it could infect if infectious itself. The average degree κ is interpreted as a measure of the level of social distancing followed by the population. For this study, we take $\kappa = 20$ and $\kappa = 40$ on a $N = 1000$ node network to consider populations with two different levels of social distancing. These values are chosen to consider two networks, one with twice as many contacts, on average, as the other. This is consistent with recent literature investigating the impacts of 50% reduction in contacts to investigate impacts of social distancing on disease transmission (Block et al., 2020).

The rewiring probability, on the other hand, gives a measure of how mixed the population is. When $p = 0$, the nodes all have exactly the same degree κ and, importantly, only interact with their nearest neighbors. This insulates "far-away" nodes from the risk of infection. Indeed, the average minimum path length between any two nodes decreases rapidly as a function of p (Newman et al., 2000). Thus, as p increases, there are fewer "far-away" nodes. The choice of p also impacts the degree distribution, in particular, increasing p increases the probability of having very high-degree nodes. We consider $p = 0.01$ and $p = 0.1$ to model populations that are less and more mixed. The lower value is representative of family and workplace networks whereas the higher value is more representative of school or university networks (Block et al., 2020; Mossong et al., 2008).

2.3   ODE model

In addition to the network model described above, we also consider the following ODE model of the disease transmission process summarized by Figure 1:

$$
\begin{aligned}
\dot{S} &= -\hat{\kappa}\beta(I + A)S - \hat{\kappa}\tau QS + \delta T_S & \dot{T}_S &= \hat{\kappa}\tau QS - \delta T_S \\
\dot{E} &= \hat{\kappa}\beta(I + A)S - \hat{\kappa}\tau QE - (\alpha_A + \alpha_I)E & \dot{T}_R &= \hat{\kappa}\tau QR - \delta T_R \\
\dot{A} &= \alpha_A E - \gamma_A A - \hat{\kappa}\tau QA & \dot{T}_Q &= \hat{\kappa}\tau(E + A + I)Q + \sigma I - \delta T_Q \\
\dot{I} &= \alpha_I E - \gamma_I I - \hat{\kappa}\tau QI - \sigma I & \dot{Q} &= \delta T_Q - \gamma_Q Q \\
\dot{R} &= \gamma_A A + \gamma_I I - \hat{\kappa}\tau QR + \delta T_R & \dot{R}_Q &= \gamma_Q Q
\end{aligned}
\tag{1}
$$

where $\hat{\kappa} = \kappa/(N - 1)$. All other ODE model parameters are the same as those given in Table 2. Our numerical simulations of the ODE model use Matlab's ode15s solver (Shampine and Reichelt, 1997).

The ODE model (1) represents the lowest-order mean field theory for approximating the average number of nodes in each state for the stochastic model on a homogeneous, uniformly random network of N nodes with degree κ. While this model does not explicitly capture details about the structure of the contact network, we can partially account for the degree of connectivity with an effective infection rate $\hat{\kappa}\beta$ based on the average degree κ of the nodes on the network. However, this correction misses the impact of heterogeneity in the degree of the nodes. Moreover, the model (1) cannot resolve the impact of the way the network connections are structured, e.g., there is no analogous way to account for the rewiring probability p. As illustrated by our results in Fig. 3, we expect ODE model to match more closely with the stochastic model for more connected ($\kappa \to N - 1$) and more well-mixed ($p \to 1$) networks.

3   Results

We use the two modeling approaches described in Section 2 to explore the impact of self-requested testing by symptomatic individuals and requisite testing of the contacts of those who test positive on disease dynamics. In Section 3.1, we compare

time series of the disease spread with different network parameters to the predictions of the ODE model. This reveals a range of behaviors in the network model that differ to varying degrees from the predictions of the ODE model with analogous parameters.

Section 3.2, we investigate the effects of the rates of contact tracing, τ, and self-reporting, σ. Simulation results from the stochastic network model and the approximate ODE model under different scenarios are presented, keeping track of several measures described below. The scenarios represent different levels of social distancing, which are related to κ, and mixing within the population, which is related to p. Under these different conditions we explore the impact of the network structure on the epidemic by examining how the following measures vary as a function of σ and τ.

- f_{100}: The fraction of outbreaks that have a minimum total infections of at least 100 individuals in the stochastic network model. In the deterministic ODE model, f_{100} will take on a value of either 0 or 1, depending on whether or not at least 100 individuals are infected during the epidemic.

- t_E: The duration of the epidemic in days, where the end of the epidemic is defined to be the time when there are no more active nodes in the network model, and when the active infectious compartments total less than 0.1 in the ODE model. Here, we consider the states E, I, A, T_Q and Q as active in the sense that they are currently, or soon to be, infected.

- N_w: The number of infection waves is calculated based on a threshold of at least 30 in the peak prominence (MathWorks-MATLAB, 2021) of active nodes.

- I_{tot}: The total number of infections during the epidemic.

- T_{tot}: The total number of tests used during the epidemic.

We note that the choice of threshold of 0.1 active nodes in definition for the end of an epidemic in t_E for the ODE model does have an impact on the results. This impact manifests itself as a sharp cutoff in the lower right of panels (c) and (f) in Figures 6-9. Because the compartments can take on arbitrarily small values in the continuous ODE model, simulations with low rates of self-reporting (small σ) and high rates of contact tracing (large τ) can lead to several infection waves with the active nodes falling to nearly zero in between. The locations of the cutoff in the (τ, σ) parameter plane depends on our choice of the threshold, which is somewhat arbitrary. This raises the questions of what it means to have a fraction of an individual infected and how small should that fraction be before we assume it cannot propagate the disease further and, at a practical level, can lead to numerical stiffness issues in simulations. This highlights a potential challenge of interpreting simulation results from ODE models when the level of infection is very low.

3.1   Time series comparisons

We first compare the time series between the stochastic network model and ODE model (1). Figure 3 considers three different pairs of parameter values, (κ, p), related to the network structure, and chooses appropriate parameters in order to obtain an equivalent ODE model. These reveal some key differences in predicted outcomes.

Panel (a), where the average degree is $\kappa = 40$ and the rewiring probability is $p = 0.1$, represents both relatively high contact and mixing. In this case, the 200 trials of the stochastic network model (light gray) appears to initially follow the predictions from the ODE model (thick blue) during the first wave of the outbreak. However, there is a significant deviation in the solutions from the network model for subsequent infection waves. The ODE model predicts a larger number of waves than does the network model.

In panel (b), the average degree is halved to $\kappa = 20$ while τ and β are doubled in order to maintain equivalent rates in the ODE model. In this case, there is less of an agreement between the two models. The ODE model over-predicts the spread of the epidemic. This over-prediction is clearly seen in panel (c) where the average degree is again set to $\kappa = 20$ but the rewiring probability is reduced by a factor of 10 to $p = 0.01$. Based on the time series, varying these parameters significantly reduces the outbreak size in the trials of the network model. With a limit on the number of possible contacts in the network model, the propagation of the disease spread can be halted under circumstances with social distancing, i.e. lower degree, and less diverse network, i.e. lower rewiring rate. This does not occur in the ODE model due to the mass action assumption.

Figure 4 shows the impact that rewiring probability p can have on the measures of interest listed at the start of Section 3 in the stochastic network model. We consider 200 trials at each (even) mean node degree $2 \leq \kappa \leq 60$ for both $p = 0.01$ and $p = 0.1$. For each κ, the parameters τ and β are adjusted in the network model so that $\hat{\tau}$ and $\hat{\beta}$ that appear in the ODE model are fixed. The ODE model thus makes the same prediction, while the median and middle quartiles based on 200 trials of the network model are shown with dashed black and shaded cyan, respectively. The minimum and maximum from the trials are also indicated by black dotted lines.

In general, increasing the degree of the network leads to more total infections I_{tot} and tests performed T_{tot}, and thus a higher fraction of outbreaks. This also leads to longer epidemics and more waves. Comparing the different rewiring rates we again observe increases in each of the measures with the higher rewiring rate. The higher rewiring rate effectively shrinks the diameter of the network and allows for faster disease spread throughout the population.

(a) $\kappa = 40, p = 0.1$ (b) $\kappa = 20, p = 0.1$ (c) $\kappa = 20\ p = 0.01$
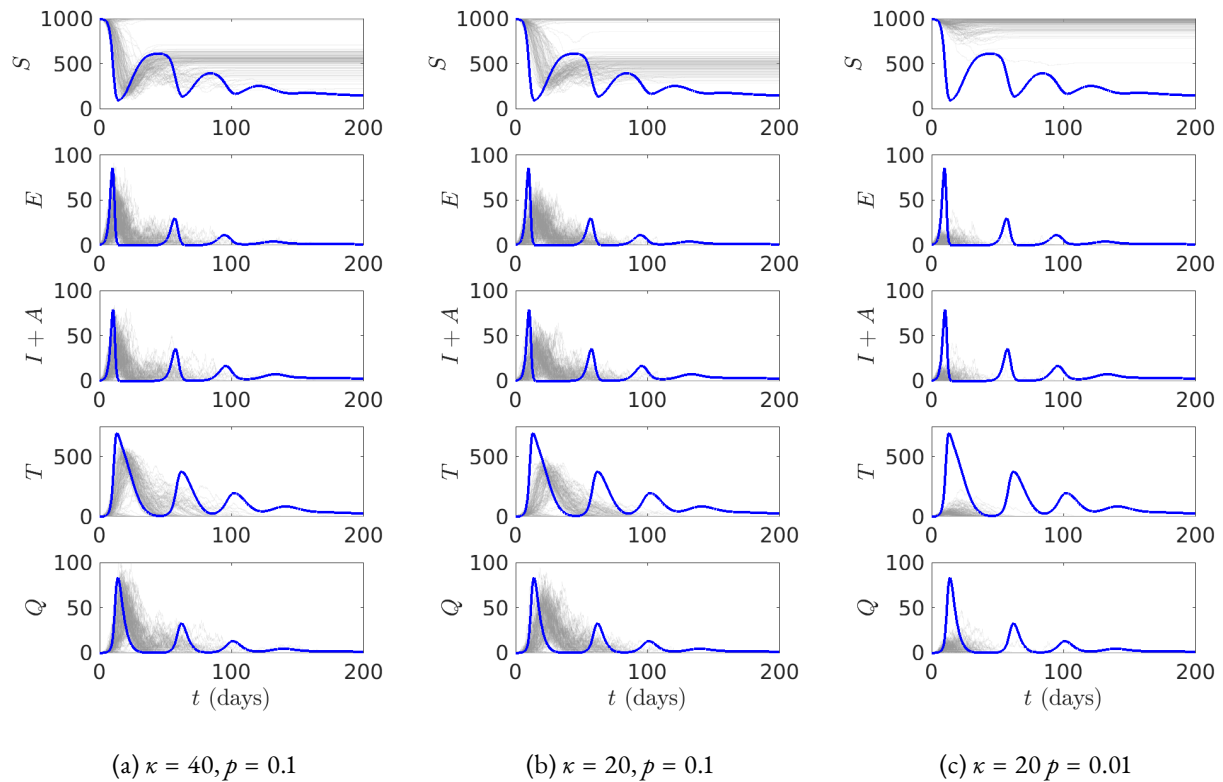
Figure 3: Comparison of predictions between the ODE model (1) with fixed parameters and the stochastic network model for different sets of network parameters: (a) $\kappa = 40$, $p = 0.1$; (b) $\kappa = 20$, $p = 0.1$; and (c) $\kappa = 20$, $p = 0.01$. In each case, the time series from a simulation of the ODE model is given by the thick blue line, and the light gray lines show each of 200 trials of the stochastic network model. Parameters are given in Table 2, except that $\sigma = 0.3$, and τ, β are adjusted to keep the ODE predictions the same across different degrees κ. In particular, $\tau = \gamma_Q \kappa_0 / \kappa$ and $\beta = \beta_0 \kappa_0 / \kappa$, where $\kappa_0 = 40$, and $\beta_0 = 0.05$. These parameters correspond to ODE simulation results in panel (f) of Figures 5-9.
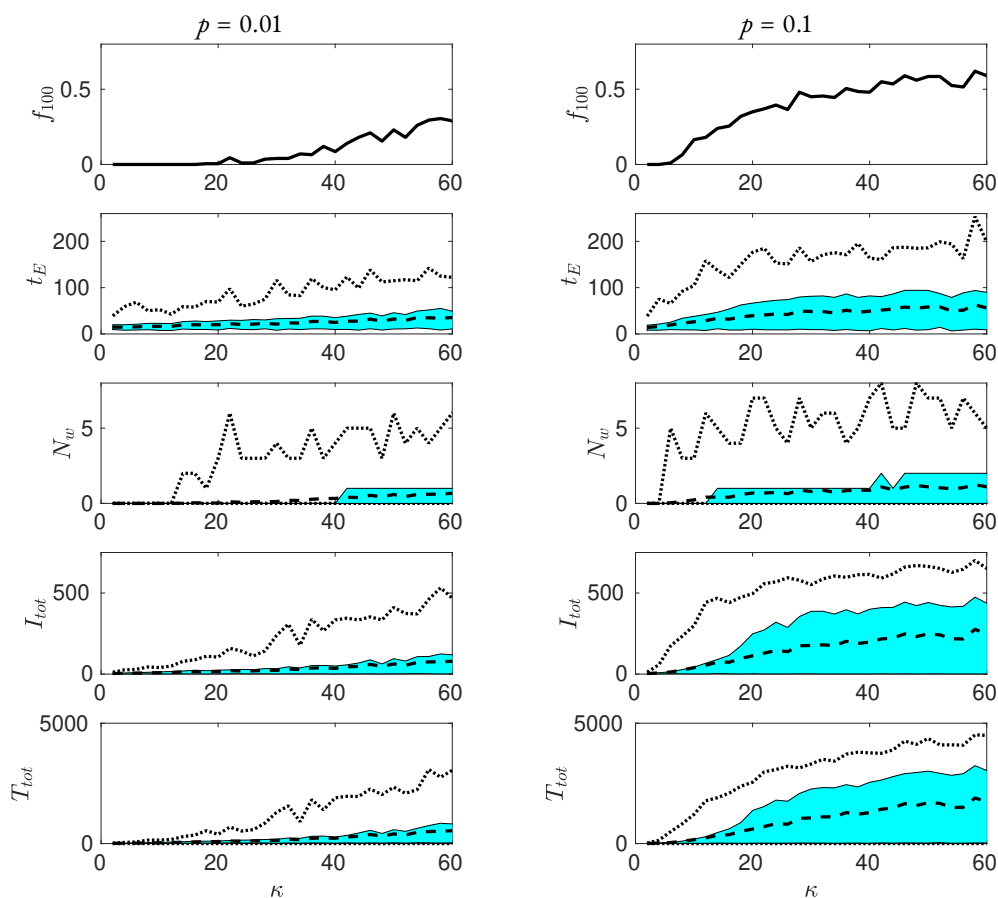
Figure 4: Comparison of the five metrics of interest discussed in Section 3 as the average degree κ of the network varies. For each degree, we run 200 simulations with N = 1000. Minimum and maximum values from simulations are shown with dotted lines, and mean values are shown in dashed lines. The cyan region is the middle 50 percent of simulations. Parameters are given in Table 2, except that σ = 0.3, and τ, β are adjusted to keep the ODE predictions the same across different degrees κ. In particular, $\tau = \gamma_Q \kappa_0 / \kappa$ and $\beta = \beta_0 \kappa_0 / \kappa$, where κ_0 = 20, and β_0 = 0.05. These parameters correspond to ODE simulation results in panel (c) of Figures 5–9. Predictions from the ODE model: t_E = 411 days, N_w = 2, I_{tot} = 757, T_{tot} = 1981 days.
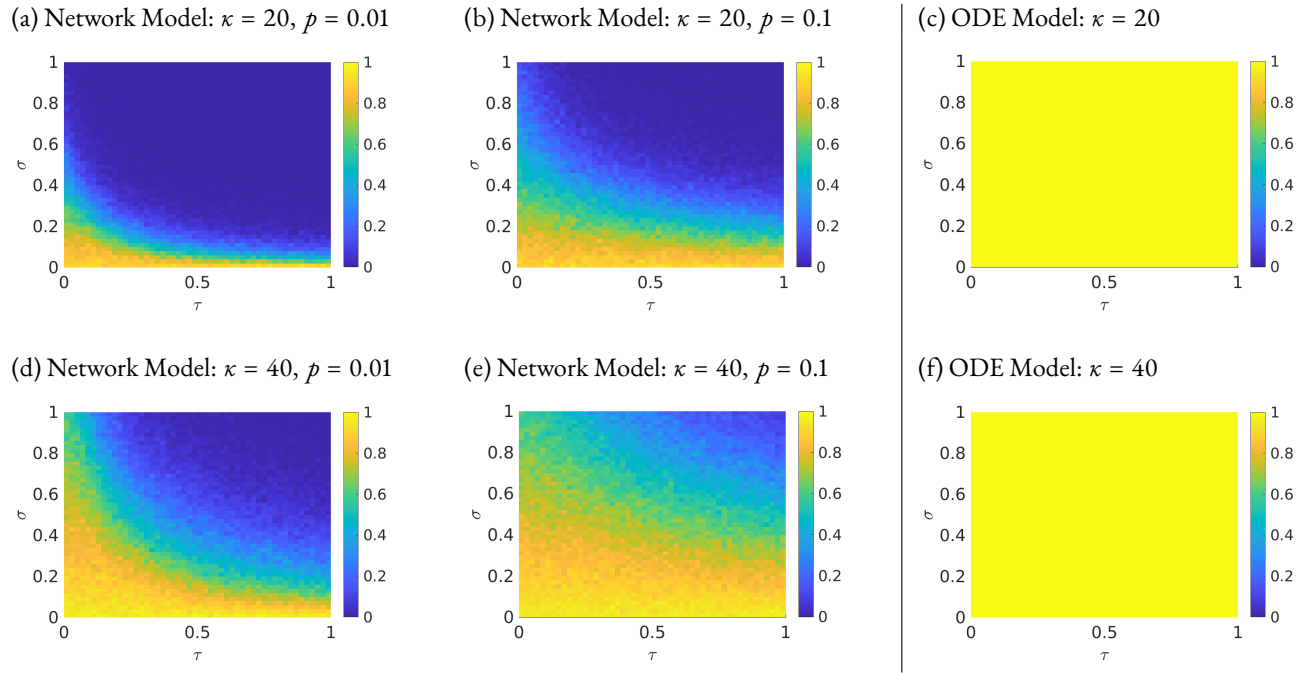
Figure 5: Simulation results for fraction of simulations f_{100} in which there is an outbreak of at least 100 cases. (a) $\kappa = 20$ and $p = 0.01$, (b) $\kappa = 20$ and $p = 0.1$, (d) $\kappa = 40$ and $p = 0.01$, and (e) $\kappa = 40$ and $p = 0.1$. (c) and (f) show results from the ODE model for $\kappa = 20$ and $\kappa = 40$, respectively.

The distribution of the number of waves N_w did not change much with the degree of the network for either value of p; however, when $p = 0.01$, the maximum value observed increased with the degree until $\kappa \geq 30$ when the maximum number of waves oscillated between $N_w = 3$ and $N_w = 5$. When $p = 0.1$, the maximum number of waves oscillated between $N_w = 3$ and $N_w = 5$ when $\kappa \geq 10$. The median and minimum value of number of waves was $N_w = 1$ for $\kappa \geq 10$ and $\kappa \geq 15$, respectively.

Overall for the lower rewiring rate, $p = 0.01$. there was a steady increase for each of the measures. On the other hand for the higher rewiring rate, $p = 0.1$, we see an initial climb in each of the measures though beyond $\kappa = 20$ to 30 the increases in the measures was much slower. This suggests that for smaller rewiring rates average degree has a larger effect on the measures than at higher rewiring rates.

3.2   Comparison of the effects of contact tracing and self-reporting

To examine the effects of contract tracing and self-reporting, we vary the associated parameters τ and σ and create plots of the measures outlined at the start of Section 3. In Figures 6–9, we consider four sets of network parameters of the stochastic network model and the two analogous cases of the ODE model. For the network model the average degree, κ, and the rewiring rate, p, are varied, whereas in the ODE model we vary only κ as the predictions do not depend on p. In cases (a), (b) and (c) the average node degree is $\kappa = 20$ ($k = 10$), which represents a scenario in which the level of social distancing is higher, whereas in cases (d), (e) and (f) the average node degree is $\kappa = 40$ ($k = 20$) so there is much less social distancing. Cases (b) and (d) have a higher rewiring rate ($p = 0.1$) than in cases (a) and (c) where the rewiring rate is $p = 0.01$. The former group represents situations where more rapid mixing can occur since these networks are less "ring-like" and more random, see Figure 2(c).

Figure 5 shows the fraction f_{100} of cases when a large outbreak (more than 100 cases total) occurs. When social distancing is the strongest and the relative mixing is the smallest (i.e., case (a)), the fraction of large outbreaks is minimal, and large outbreaks only occur when there is essentially no self reporting or when both testing rates and self-reporting rates are very low. On the other hand when social distancing is weaker and the relative mixing is strong (i.e., case (d)), the chances of a large outbreak is much greater. In fact a large outbreak occurs almost every time when the self-reporting rate σ is less than $1/2$ regardless of the rate of testing, which suggests that even large rates of testing cannot compensate for a lack of self-reporting when mixing is high and social distancing is low.

If rates of testing and self-reporting are both high, however, it is still possible to avoid large outbreaks. In the intermediate cases (i.e., cases (b) and (c)), we found that doubling the average degree has a larger effect on the fraction of outbreaks that are large than does increasing the rewiring rate p by a factor of 10. When the average degree κ is doubled, more large outbreaks occurred when the rate of testing was low for both values of p considered, and the relationships between the fraction of large
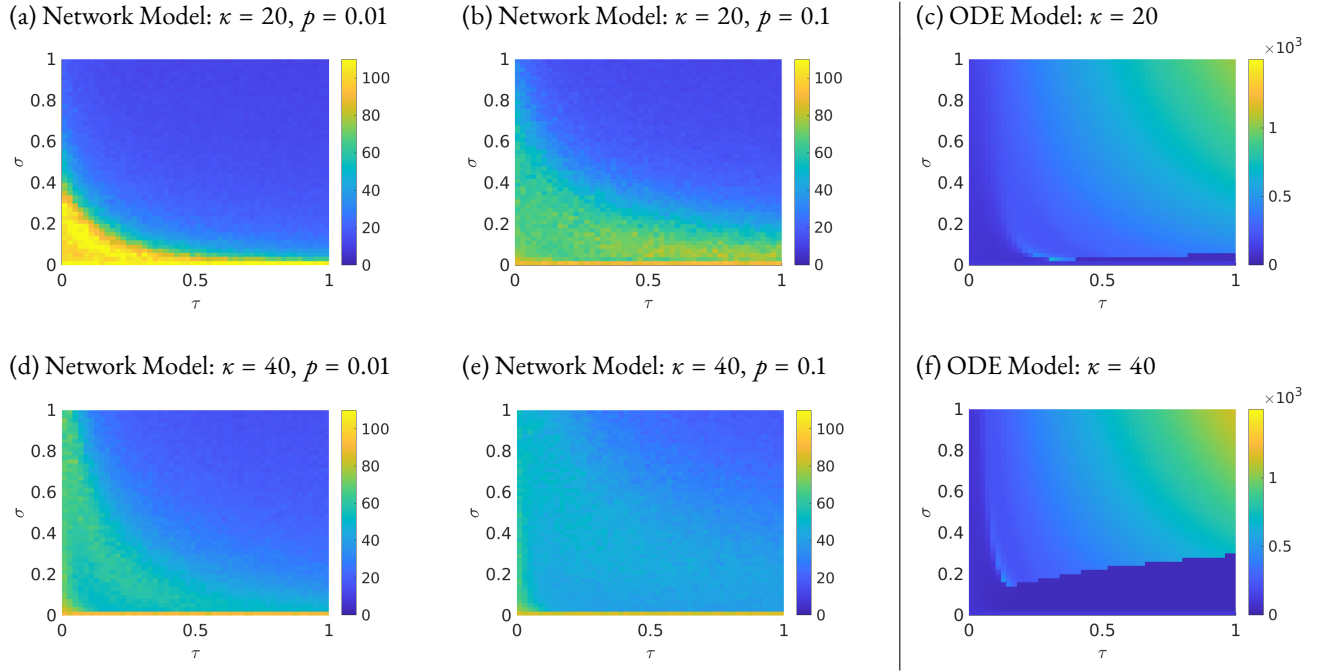
Figure 6: Simulation results for total length in time t_E of the epidemic in days. (a) $\kappa = 20$ and $p = 0.01$, (b) $\kappa = 20$ and $p = 0.1$, (d) $\kappa = 40$ and $p = 0.01$, and (e) $\kappa = 40$ and $p = 0.1$. (c) and (f) show results from the ODE model when $\kappa = 20$ and $\kappa = 40$, respectively.

outbreaks f_{100} and the parameters σ and τ become substantially more nonlinear, in particular when the rewiring probability is low. Due to the smaller amount of mixing, increasing both σ and τ will more likely decrease the chances of a large outbreak, whereas with the higher mixing rate increasing the self-reporting rate alone has the largest effect.

For the ODE model we see that there is always an outbreak, see (c) and (f) in Figure 5. This is due to the lack of structure in this model. In the network model the disease can end when infected nodes have no susceptible nodes to infect due to the lack of connections as well as to effective contact tracing. This does not happen in the ODE model due to assumption that the population is well mixed.

Figure 6 demonstrates the importance of self-reporting and contact tracing in determining the duration t_E of the epidemic. In the network model t_E is quantified by the number of days until there are no more infectious individuals. The epidemic runs unabated for long durations at low σ and low τ for all network parameters considered. Under stronger social distancing, $\kappa = 20$, the self-reporting rate appears to have more effect than the contact tracing, whereas in the weaker social distancing case, $\kappa = 40$, their effects are comparable in reducing t_E.

For the ODE model we define the epidemic time t_E to be when the number of infectious is less than 0.1. Here we see the opposite behavior from the results of the network model: the length of the epidemic increases as the rates of contact tracing and self-reporting increase. Again because of the lack of structure within the ODE model the epidemic is allowed to continue due to all of the allowed connection being present between individuals. As the rates increase this slows down the epidemic spread, however, the disease will not stop until everyone has been infected. We note that the sharp cutoff in the lower part of panels (c) and (f) associated to the ODE model result from the definition that an epidemic ends after the active nodes fall below a total of 0.1. Above the sharp cutoff, the simulation never falls below the threshold of 0.1 between any of the waves. Below the threshold, we see cases where the active nodes fall below 0.1 after the first wave, but additional waves would be possible in the continuous ODE model where the active nodes can fall arbitrarily close to zero before starting a new wave. Lowering the choice of threshold, allows the trends above the cutoff to continue further down in the graph, effectively pushing the cutoff lower. The effect of the threshold here also manifests in panels (c) and (f) in Figures 7, 8 and 9 below.

As previously mentioned it is possible to observe multiple waves over time. In Figures 7 (c) and (f) and in Figure 3 we see multiple waves in the ODE approximations of the network model, though there are typically fewer realized in the network model. The number of waves generally increase as the contact tracing rate increase, especially for low- to mid-level rates of self-reporting.

In Figures 7 (a), (b), (d) and (e) we see that the average number of the waves N_w for the network simulations are typically one or less. The cases where there is at least one wave on average occur for low values of σ and τ, however in the case with higher node degree and rewiring rates we generally see at least one wave for values of σ or τ less than 0.5.

Examining the results of the ODE model show that there tend to be more waves with higher levels of contact tracing. This
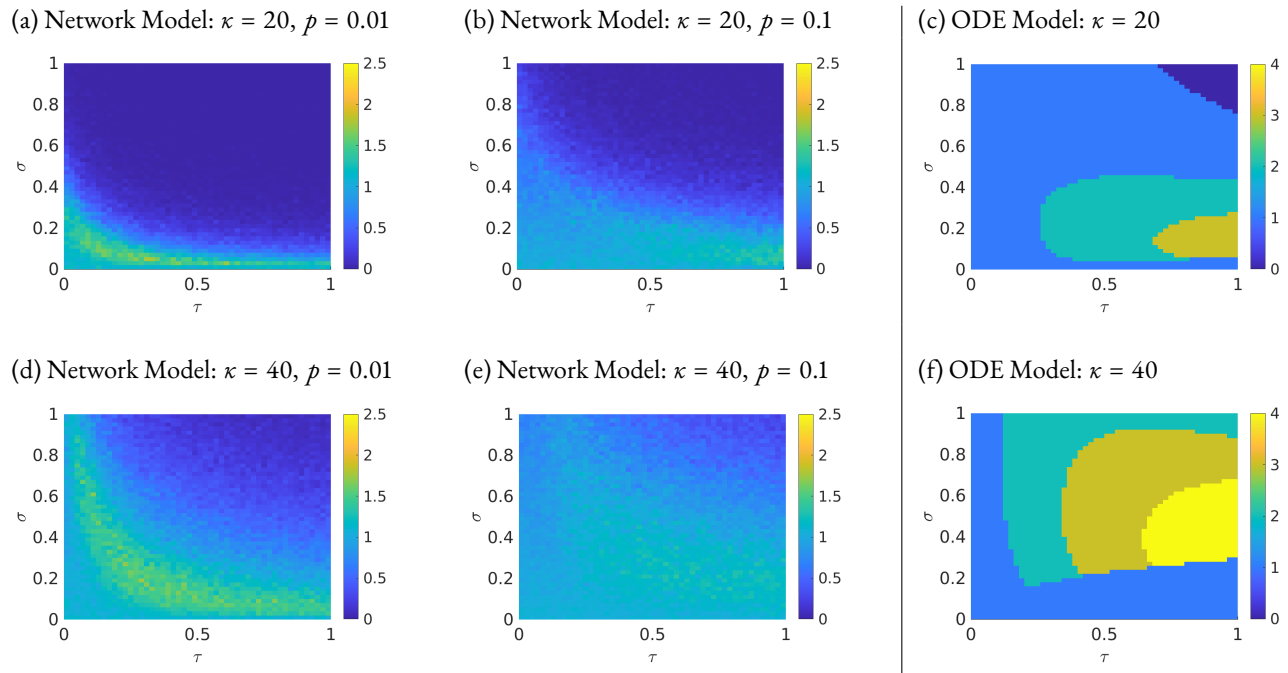
Figure 7: Simulation results for the average number N_w of waves occurring in the simulations. (a) $\kappa = 20$ and $p = 0.01$, (b) $\kappa = 20$ and $p = 0.1$, (d) $\kappa = 40$ and $p = 0.01$, and (e) $\kappa = 40$ and $p = 0.1$. (c) and (f) show results from the ODE model when $\kappa = 20$ and $\kappa = 40$, respectively.

is especially true for lower rates of self-reporting with the smaller $\kappa = 20$, and generally true for self-reporting rates above 0.2 for $\kappa = 40$. For the most part the region of the parameter space with higher N_w are disjoint when comparing the network and ODE models, and hence give very different results.

An important measure in epidemics involves the total number I_{tot} of cases of infections within a population, see Figure 8. For the case where there is more social distancing, self-reporting is critical in order to keep I_{tot} down. In the case where there is less social distancing, increasing contact tracing becomes more critical in keeping the total number of infections down. Alternatively, in the case with less social distancing and a higher rewiring rate, $\kappa = 40$ and $p = 0.1$, we essentially need to require $\sigma, \tau > 0.5$ in order to keep the total number of infections below 50% of the population.

For the ODE model we observe more complicated behavior. In the case with a higher level of social distancing, Figure 8 (c), this behaves more similarly to the network models where increasing both contact tracing and self-reporting is important to keep the percent of the population infected low. On the other hand in Figure 8 (f), due to the increase of the number of connections between individuals it is nearly impossible to prevent the disease spreading to the entire population. The only region where essentially not everyone gets infected is with low self-reporting and moderate to high levels of contact tracing. We point out that for these simulations our condition of having the simulations stop at 0.1 infected people can result different answers if the simulations are allowed to continue. This is because in the continuous model the levels can drop very low but the disease can still progress over long periods of time and eventually infect the entire population.

Figure 9 presents the number T_{tot} of tests performed over the entire epidemic. This can be used in cost estimates of conducting contact tracing during an epidemic. Tracking the total number of tests varies nonlinearly with both the self-reporting rate, σ, and the contact tracing rate, τ. In the network model when $\kappa = 20$ and $p = 0.01$ not many tests are preformed, and the maximum number of tests occur when the self-reporting rate is low and contact tracing is moderate to high. This is due to the structure of the network since we see that in Figure 5, the likelihood of the epidemic spread is small and only occurs for low values of the self-reporting rate. It also suggests that, depending on self-testing rates, it may be possible to reduce the overall cost by increasing resources towards contact tracing.

Again considering the network model at the other end of the spectrum with higher node degree, $\kappa = 40$, and higher mixing rates, $p = 0.1$, we see that most individuals get tested when the self-reporting rate is low to moderate and the contact tracing rate is moderate to high. In most cases the number of tests decrease when the self-reporting rate increase beyond 50%.

Not surprisingly, as the contact tracing rate increases the total number of tests performed increases. However, generally the total number of tests tend to decrease, after reaching a maximum, as the self-reporting rate increases. This makes a case that educating the public to get tested is critical both to decreasing the likelihood of an epidemic occurring but also as a way to keep costs down.
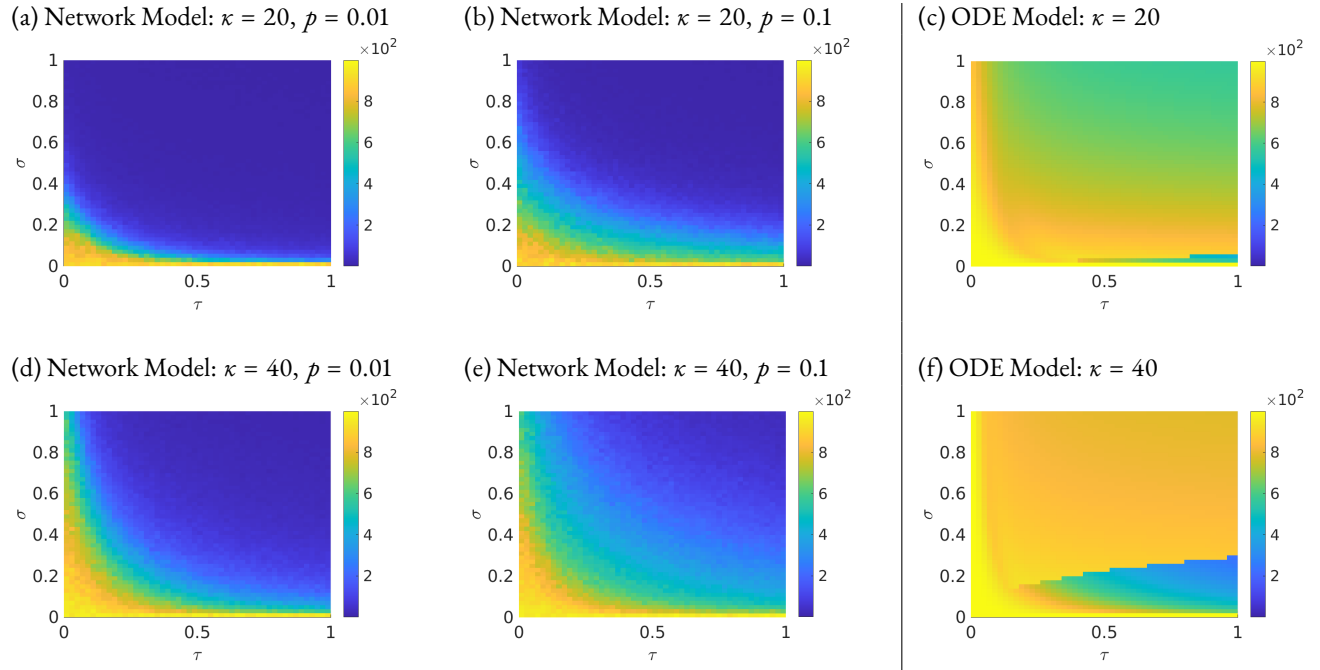
Figure 8: Simulation results for total number I_{tot} of people infected. (a) $\kappa = 20$ and $p = 0.01$, (b) $\kappa = 20$ and $p = 0.1$, (d) $\kappa = 40$ and $p = 0.01$, and (e) $\kappa = 40$ and $p = 0.1$. (c) and (f) show results from the ODE model when $\kappa = 20$ and $\kappa = 40$, respectively.
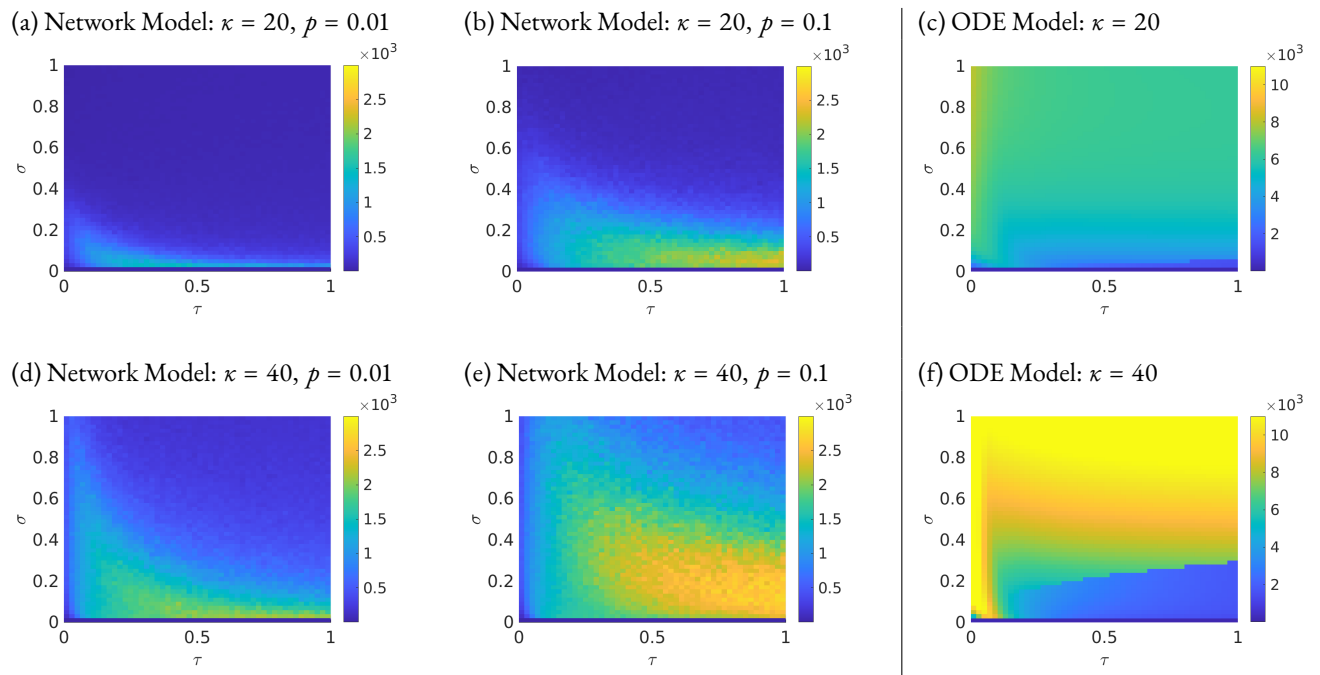
Figure 9: Simulation results for total number T_{tot} of tests performed. (a) $\kappa = 20$ and $p = 0.01$, (b) $\kappa = 20$ and $p = 0.1$, (d) $\kappa = 40$ and $p = 0.01$, and (e) $\kappa = 40$ and $p = 0.1$. (c) and (f) show results from the ODE model when $\kappa = 20$ and $\kappa = 40$, respectively.

The ODE model reveals very different behavior. As the self-reporting rate increases so do the number of tests performed. The contact tracing rate has little effect in these cases which is counter-intuitive. The only effect occurs when contact tracing is essentially non-existent which results in increasing the number of tests performed. One does see throughout Figure 9 that repetitive testing is occurring since the maximum counts can be above the total population of 1,000. This occurs in both models, and appears to be more frequent in the ODE models.

4   Discussion

Limiting outbreaks during an epidemic with the presence of asymptomatic spread is difficult in general. However, once an individual has been identified as infectious, contact tracing aids in limiting spread by testing and isolating those who have a significant chance of having been infected. Applying resources toward the tracing process can increase the rate at which contacts can be tested, and thus more quickly identify infections. Since the process cannot be initiated until an infected person is identified, the rate at which symptomatic individuals decide to get tested plays a key role in the overall success of the contact tracing process. In this study, we explored the interplay between rates of contact tracing of an infected individual and how likely someone showing symptoms will get tested in controlling an epidemic.

We constructed a stochastic network model to explore tracing and testing protocols within an epidemic, and compared the results to an analogous ODE model based on the assumption of a well-mixed population. The contact tracing process is tied to the structure of regular contacts between individuals in the population. It is not surprising that the predictions of an ODE model with an underlying assumption of a well-connected and well-mixed population are very different from a network approach that explicitly captures the details of this contact structure. This result in particular is one that has been observed in other comparisons of explicit network models and their ODE approximations (Müller and Kretzschmar, 2021). Our focus is on examining the interaction between rates of self-reporting and contact tracing on different measures under various network structures. We carried out simulations over a range of parameters, and calculated resulting measures of interest over realizations of a Watts-Strogatz random network. We considered high and low values of the mean degree κ, which relates to how well-connected the population is, as well as low and high values of the rewiring probability p, which relates to how well-mixed the population is.

The rate of testing, σ, which characterizes the rate at which infected individuals self-report symptoms and get tested, and the rate of the contact tracing, τ, which characterizes the rate at which contacts of a quarantined individual are tested, have different effects in our simulations of the network model. Generally the self-reporting rate, σ, is critical to controlling the progress of the spread of the epidemic. Clearly the process of contact tracing cannot be effective if there is no self-reporting occurring due to the lack of targets for contact tracing. When self-reporting is occurring, having the contact tracing rate above some minimal rate, around 30% of a quarantined node's contacts per day (based on our set of parameters), resulted in a positive effect on the decreasing the spread of the epidemic in the network model. Contract tracing at and above this threshold resulted in decreases in the chance of having an outbreak, epidemic time, and number of waves. The total number of tests, on the other hand, did not vary monotonically with these parameters. There is a "hump" that, if overcome, can actually reduce the overall number of tests used by sufficiently curbing the spread of the disease and reducing the size of the outbreak. Thus, near the parameters associated with the hump, putting more resources into tracing and encouraging self-reporting of symptoms has the potential to actually reduce the overall cost of the control measures.

Results from the ODE model follow different, and in some cases contrary, qualitative trends from the network model. The differences are due to a few factors including model choice. The ODE model works on a continuous variable unlike the network model, which complicates the stopping criteria for the epidemic. The fact that the number of active individuals never falls to exactly zero contributes to the contrary results relative to the network model. This is in part due to the decision of how to define the end of the epidemic. The choice of threshold level for ending the epidemic has impact on measures of interest, as seen by the sharp cut-offs in panels (c) and (f) of Figures 6–9. The specific threshold level controls the location of this sharp cutoff, but the epidemic can persist for any nonzero threshold value since new waves can develop from an arbitrarily small level of infections given small enough σ and large enough τ.

Additionally, due to the assumption of mass action, a large fraction of the susceptibles are pulled into isolation as contacts of more quarantined individuals are tested. This reduces the available population to spread of the disease and consequently extinguishes the outbreak. However, once the quarantined population returns to being susceptible, an extremely small level of infection may be enough to initiate another wave and restart the process. The ODE model tends to produce more waves since some level of infection always remains to act as a potential seed for the next wave. We also note that the structure of the waves seen in the ODE time series plots of Figure 3 suggests fast-slow dynamics may be at play (Wechselberger, 2020; Schecter, 2021; Jardón-Kojakhmetov et al., 2021). This may provide a path forward for analysis of the ODE model, particularly in the low σ and high τ regime where waves can be initiated by vanishingly small levels of infection.

Epidemic waves are often a part of an emerging infectious disease, and have in fact been observed during the recent COVID-19 pandemic (Dong et al., 2020). These waves occurred when large numbers of individuals were reintroduced to public areas where

exposure to infectious people can occur. This often occurred during holidays when people gathered, or when restrictions were removed or eased, or even when a new variant started spreading within the population. These waves then slowed down as the susceptible population is depleted and as restrictions are reinforced (Hale et al., 2021). Although we are not modeling this situation in our work, the dynamics are similar. We did not account for changes in human behavior during or in response to the epidemic beyond quarantine and isolation as a result of testing and tracing. However, similar infection waves have been also been observed in ODE models in which individuals switch to behaviors that reduce disease transmission in response to high levels of infection (Poletti et al., 2009; Schecter, 2021). A network approach may be able to capture more details of this process as individual behaviors are often strongly influenced by those they come into regular contact with. Future work could incorporate behavioral changes into our model to assess the impact of interactions between these changes, testing, and tracing. Those making policy decisions as well as those modelers assisting policy makers should carefully consider the models and how decisions are make based on those models.

Numerous studies have investigated contact tracing in network, ODE, and branching process models (Müller and Kretzschmar, 2021; Kwok et al., 2019). In one of the first theoretical analyses of contact tracing in network models, the authors explored relationships between the efficiency of contact tracing and the basic reproductive number R_0 and showed that the relationship between contact tracing efficiency and R_0 held under a variety of scenarios except when high levels of clustering occurred in a network (Eames and Keeling, 2003). Armbruster and Brandeau (2007) investigated the cost-effectiveness of contact tracing with and without additional screening and found increases in tracing may have diminishing returns in reducing disease prevalence in a population. In Shahtori et al. (2018), the authors showed that contact tracing and rapid hospitalization early in an Ebola outbreak has a significant impact on reducing cases compared to tracing that begins later in an outbreak, a result which our results support given that higher rates of self-reporting and willingness to get tested lead to earlier detection and quarantine of cases. In recent work looking at COVID-19 control via contact tracing, Bradshaw et al. (2021) showed that bi-directional contact tracing aimed at identifying both potential infectors and infectees was more effective than uni-directional contact tracing that targets only potential infectees, and Firth et al. (2020) showed that tracing contacts of contacts may also be a better approach than targeting only potential infectees that interact with an index case. Both of these approaches, like our work, emphasizes that strategies aimed at detecting asymptomatic cases in addition to symptomatic cases is critical for disease control with the existence of asymptomatic cases. Additionally, our study contributes to this body of literature a novel exploration of the role of contact tracing and self-testing and the interactions between the two in infectious disease control and how network structure, or the lack thereof, impacts the efficacy of testing and tracing. Importantly, we show that the willingness to self-report and the process of contacts getting traced each are important to the efficacy of contact tracing. This emphasizes that educating people on the importance of getting tested when initial symptoms begin or when a possible exposure has occurred is critical to control an emerging infectious disease outbreak. This is clearly of critical importance for policy makers though can be very challenging when dealing with a wary public.

We have made a number of simplifying assumptions in the stochastic network model which may be interesting to relax. We assumed perfectly accurate tests, complete compliance with quarantine while awaiting test results and with isolation if tested positive. In reality we expect testing errors, and the accuracy levels may depend on the time for test results to be available. Moreover, this trade-off between accuracy and wait-time may be influenced by the levels of failure to comply with isolation and quarantine protocols. A more detailed model of the tracing process that includes capacity limits on the total number of contacts that can be traced at a given time may provide more insight into the cost-benefit analysis for the optimal usage of resources. We also did not include surveillance or mandatory testing, which may allow for earlier initiation of contact tracing, but at the cost of testing the population at large instead of only those closest to infected individuals. We assumed throughout a fixed ratio of 6:1 symptomatic to asymptomatic cases. This choice was made to explore a scenario where a relatively small fraction of cases are asymptomatic, and we expect that a higher probability of asymptomatic cases would increase the impact that contact tracing can have relative to self-reporting, and would be interesting to explore further in future work. Furthermore, We modeled contacts among individuals with an idealized random network structure because of its simplicity and flexibility, but a network that more closely mimics actual human contact structure within a population may have different trends. Other networks based on models of societal structure and predicted human behavior could be explored as has been done by Eames et al. (2012); Kucharski et al. (2018); Della Rossa et al. (2020). Efforts to directly estimate the contact structure from mobility data may also inform improved models for network structure and suggest how it changes in different scenarios (Wesolowski et al., 2016; Kishore et al., 2020; Buckee et al., 2020).

The discrepancy between the predictions of the stochastic network model and the ODE model in our work highlights the importance of model choice when conducting studies especially in cases for making policy. The network model, while it includes more details of interactions between individuals, is significantly more complex than the ODE model and requires more computational resources to explore. On the other hand, the ODE model does not capture details of the structure of contacts between individuals, and thus may miss key insights into the effectiveness of contact tracing at controlling an epidemic. We show some contradicting conclusions based on the type of model used. These include the presence of a minimum threshold for contact tracing for outbreaks in only the network model. The length of the epidemic, the number of people infected, and the number

of tests used have a reverse quality with respect to the contact tracing rate between the models. These are relevant quantities in terms of decision making during pandemics.

Advances in the development of ODE models that capture more details about the influence of network structure may provide a middle ground between existing ODE models and more complex network models (Kiss et al., 2017; Jardón-Kojakhmetov et al., 2021). Such mean-field models are based on higher-order moment closures, and explicitly track mean levels of edge types (where the type is determined by which states the edge connects) in addition to the mean levels of each state. This kind of extension could be incorporated into a model for contact tracing where the overall tracing rate at any given time is proportional to the number of edges where one node is in quarantine. It would allow for an ODE model that can capture some aspects of the contact network structure, such as the impact of the rewiring parameter p. This comes at the expense of tracking additional state variables related to how the network is connected. Still though, these models would likely not highlight the importance of network structure and interactions at the individual level, and these models remain preferable to ODE approximations, particularly when the population being studied is relatively small.

Acknowledgments

References

Armbruster, B. and M. L. Brandeau (2007). Contact tracing to control infectious disease: when enough is enough. *Health care management science 10*(4), 341–355. 23, 36

Arunkumar, G., R. Chandni, D. T. Mourya, S. K. Singh, R. Sadanandan, P. Sudan, and B. Bhargava (2019). Outbreak investigation of Nipah virus disease in Kerala, India, 2018. *The Journal of infectious diseases 219*(12), 1867–1878. 23

Azizi, A., C. Montalvo, B. Espinoza, Y. Kang, and C. Castillo-Chavez (2020). Epidemics on networks: Reducing disease transmission using health emergency declarations and peer communication. *Infectious Disease Modelling 5*, 12–22. 24

Block, P., M. Hoffman, I. J. Raabe, J. B. Dowd, C. Rahal, R. Kashyap, and M. C. Mills (2020). Social network-based distancing strategies to flatten the COVID-19 curve in a post-lockdown world. *Nature Human Behaviour 4*(6), 588–596. 27

Bradshaw, W. J., E. C. Alley, J. H. Huggins, A. L. Lloyd, and K. M. Esvelt (2021). Bidirectional contact tracing could dramatically improve COVID-19 control. *Nature communications 12*(1), 1–9. 24, 36

Buckee, C. O., S. Balsari, J. Chan, M. Crosas, F. Dominici, U. Gasser, Y. H. Grad, B. Grenfell, M. E. Halloran, M. U. Kraemer, et al. (2020). Aggregated mobility data could help fight COVID-19. *Science 368*(6487), 145–147. 36

CDC (2022a). COVID-19. Accessed 29-March-2022. 26

CDC (2022b). Key facts about influenza (flu). Accessed 29-March-2022. 26

Cope, R. C., J. V. Ross, M. Chilver, N. P. Stocks, and L. Mitchell (2018). Characterising seasonal influenza epidemiology using primary care surveillance data. *PLoS computational biology 14*(8), e1006377. 26

Cowan, F. M., R. French, and A. M. Johnson (1996). The role and effectiveness of partner notification in STD control: a review. *Genitourinary medicine 72*(4), 247. 23

Della Rossa, F., D. Salzano, A. Di Meglio, F. De Lellis, M. Coraggio, C. Calabrese, A. Guarino, R. Cardona-Rivera, P. De Lellis, D. Liuzza, et al. (2020). A network model of Italy shows that intermittent regional strategies can alleviate the COVID-19 epidemic. *Nature communications 11*(1), 1–9. 36

Dhillon, R. S. and D. Srikrishna (2018). When is contact tracing not enough to stop an outbreak? *The Lancet Infectious Diseases 18*(12), 1302–1304. 23

Dong, E., H. Du, and L. Gardner (2020). An interactive web-based dashboard to track COVID-19 in real time. *The Lancet infectious diseases 20*(5), 533–534. 35

Donnelly, C. A., A. C. Ghani, G. M. Leung, A. J. Hedley, C. Fraser, S. Riley, L. J. Abu-Raddad, L.-M. Ho, T.-Q. Thach, P. Chau, et al. (2003). Epidemiological determinants of spread of causal agent of severe acute respiratory syndrome in Hong Kong. *The Lancet 361*(9371), 1761–1766. 23

Eames, K. T. and M. J. Keeling (2003). Contact tracing and disease control. *Proceedings of the Royal Society of London. Series B: Biological Sciences 270*(1533), 2565–2571. 23, 36

Eames, K. T., N. L. Tilston, E. Brooks-Pollock, and W. J. Edmunds (2012). Measured dynamic social contact patterns explain the spread of H1N1v influenza. *PLoS computational biology 8*(3), e1002425. 36

Firth, J., J. Hellewell, P. Klepac, S. Kissler, A. Kucharski, and L. Spurgin (2020, 10). Using a real-world network to model localized COVID-19 control strategies. *Nature Medicine 26*, 1616–1622. 24, 36

GitHub (2022). Sample MATLAB code for simulating network model and comparing to ODE model. `https://github.com/PunitGandhi/ContactTracing.git`. 26

Hale, T., N. Angrist, A. J. Hale, B. Kira, S. Majumdar, A. Petherick, T. Phillips, D. Sridhar, R. N. Thompson, S. Webster, et al. (2021). Government responses and COVID-19 deaths: Global evidence across multiple pandemic waves. *PloS one 16*(7), e0253116. 36

Hethcote, H. W. and J. A. Yorke (2014). *Gonorrhea transmission dynamics and control*, Volume 56. Springer. 23

Hyman, J. M., J. Li, and E. A. Stanley (2003). Modeling the impact of random screening and contact tracing in reducing the spread of HIV. *Mathematical biosciences 181*(1), 17–54. 23

Jardón-Kojakhmetov, H., C. Kuehn, A. Pugliese, and M. Sensi (2021). A geometric analysis of the SIRS epidemiological model on a homogeneous network. *Journal of mathematical biology 83*(4), 1–38. 35, 37

Karaivanov, A. (2020). A social network model of COVID-19. *Plos one 15*(10), e0240878. 23, 24

Keeling, M. J. and P. Rohani (2011). *Modeling infectious diseases in humans and animals*. Princeton university press. 24

Kishore, N., M. V. Kiang, K. Engø-Monsen, N. Vembar, A. Schroeder, S. Balsari, and C. O. Buckee (2020). Measuring mobility to monitor travel and physical distancing interventions: a common framework for mobile phone data analysis. *The Lancet Digital Health 2*(11), e622–e628. 36

Kiss, I. K., J. C. Miller, and P. L. Simon (2017). *Mathematics of Epidemics on Networks*, Volume 46. Springer. 25, 37

Klinkenberg, D., C. Fraser, and H. Heesterbeek (2006). The effectiveness of contact tracing in emerging epidemics. *PloS one 1*(1), e12. 23

Kucharski, A. J., P. Klepac, A. J. Conlan, S. M. Kissler, M. L. Tang, H. Fry, J. R. Gog, W. J. Edmunds, J. C. Emery, G. Medley, et al. (2020). Effectiveness of isolation, testing, contact tracing, and physical distancing on reducing transmission of SARS-CoV-2 in different settings: a mathematical modelling study. *The Lancet Infectious Diseases 20*(10), 1151–1160. 26

Kucharski, A. J., C. Wenham, P. Brownlee, L. Racon, N. Widmer, K. T. Eames, and A. J. Conlan (2018). Structure and consistency of self-reported social contact networks in British secondary schools. *PLoS one 13*(7), e0200090. 36

Kwok, K. O., A. Tang, V. W. Wei, W. H. Park, E. K. Yeoh, and S. Riley (2019). Epidemic models of contact tracing: systematic review of transmission studies of severe acute respiratory syndrome and Middle East respiratory syndrome. *Computational and structural biotechnology journal 17*, 186–194. 36

Lessler, J., N. G. Reich, R. Brookmeyer, T. M. Perl, K. E. Nelson, and D. A. Cummings (2009). Incubation periods of acute respiratory viral infections: a systematic review. *The Lancet infectious diseases 9*(5), 291–300. 26

MacIntyre, C. R. (2020). Case isolation, contact tracing, and physical distancing are pillars of COVID-19 pandemic control, not optional choices. *The Lancet Infectious Diseases 20*(10), 1105–1106. 23

MathWorks-MATLAB (2021). findpeaks. Retrieved October 8th, 2021 from `https://www.mathworks.com/help/signal/ref/findpeaks.html#buff2t6`. 28

Mossong, J., N. Hens, M. Jit, P. Beutels, K. Auranen, R. Mikolajczyk, M. Massari, S. Salmaso, G. S. Tomba, J. Wallinga, et al. (2008). Social contacts and mixing patterns relevant to the spread of infectious diseases. *PLoS medicine 5*(3), e74. 27

Müller, J. and M. Kretzschmar (2021). Contact tracing–old models and new challenges. *Infectious Disease Modelling 6*, 222–231. 23, 35, 36

Newman, M. E., C. Moore, and D. J. Watts (2000). Mean-field solution of the small-world network model. *Physical Review Letters 84*(14), 3201. 27

Poletti, P., B. Caprile, M. Ajelli, A. Pugliese, and S. Merler (2009). Spontaneous behavioural changes in response to epidemics. *Journal of theoretical biology 260*(1), 31–40. 36

Ramstedt, K., G. Hallhagen, B.-I. Lundin, C. Håkansson, G. Johannisson, G. Löwhagen, G. Norkrans, and J. Giesecke (1990). Contact tracing for human immunodeficiency virus (HIV) infection. *Sexually transmitted diseases 17*(1), 37–41. 23

Schecter, S. (2021). Geometric singular perturbation theory analysis of an epidemic model with spontaneous human behavioral change. *Journal of Mathematical Biology 82*(6), 1–26. 35, 36

Shaban, N., M. Andersson, Å. Svensson, and T. Britton (2008). Networks, epidemics and vaccination through contact tracing. *Mathematical biosciences 216*(1), 1–8. 24

Shahtori, N. M., T. Ferdousi, C. Scoglio, and F. D. Sahneh (2018). Quantifying the impact of early-stage contact tracing on controlling ebola diffusion. *Mathematical Biosciences & Engineering 15*(5), 1165. 36

Shampine, L. F. and M. W. Reichelt (1997). The MATLAB ODE suite. *SIAM journal on scientific computing 18*(1), 1–22. 27

Steinbrook, R. (2020). Contact tracing, testing, and control of COVID-19—learning from Taiwan. *JAMA internal medicine 180*(9), 1163–1164. 23

Tsimring, L. S. and R. Huerta (2003). Modeling of contact tracing in social networks. *Physica A: Statistical Mechanics and its Applications 325*(1), 33–39. Stochastic Systems: From Randomness to Complexity. 24

Tupper, P., H. Boury, M. Yerlanov, and C. Colijn (2020). Event-specific interventions to minimize COVID-19 transmission. *Proceedings of the National Academy of Sciences 117*(50), 32038–32045. 26

Watts, D. J. and S. H. Strogatz (1998). Collective dynamics of 'small-world' networks. *nature 393*(6684), 440–442. 25

Wechselberger, M. (2020). *Geometric singular perturbation theory beyond the standard form*. Springer Nature. 35

Wesolowski, A., C. O. Buckee, K. Engø-Monsen, and C. J. E. Metcalf (2016). Connecting mobility to infectious diseases: the promise and limits of mobile phone data. *The Journal of infectious diseases 214*(suppl_4), S414–S420. 36

WHO (2020). Coronavirus. `https://www.who.int/health-topics/coronavirus#tab=tab_1`. 23

World Health Organization et al. (2014). Ebola and Marburg virus disease epidemics: preparedness, alert, control, and evaluation. Technical report, World Health Organization. 23